Review of Hydrodynamic Scaling Laws in Aquatic Locomotion and Fishlike Swimming

M. S. Triantafyllou

F. S. Hover

A. H. Techet

D. K. P. Yue

Department of Ocean Engineering,
Massachusetts Institute of Technology,
Cambridge, MA 02139

We consider observations and data from live fish and cetaceans, as well as data from engineered flapping foils and fishlike robots, and compare them against fluid mechanics based scaling laws. These laws have been derived on theoretical/numerical/experimental grounds to optimize the power needed for propulsion, or the energy needed for turning and fast starting. The rhythmic, oscillatory motion of fish requires an "impedance matching" between the dynamics of the actively controlled musculature and the fluid loads, to arrive at an optimal motion of the fish's body. Hence, the degree to which data from live fish, optimized robots, and experimental apparatus are in accordance with, or deviate from these flow-based laws, allows one to assess limitations on performance due to control and sensing choices, and material and structural limitations. This review focuses primarily on numerical and experimental studies of steadily flapping foils for propulsion; three-dimensional effects in flapping foils; multiple foils and foils interacting with bodies; maneuvering and fast-starting foils; the interaction of foils with oncoming, externally-generated vorticity; the influence of Reynolds number on foil performance; scaling effects of flexing stiffness of foils; and scaling laws in fishlike swimming. This review article cites 117 references. [DOI: 10.1115/1.1943433]

1 Introduction

Many autonomous underwater vehicles (AUV) used for ocean exploration and mapping have similar size and mass to marine animals. Fish and marine mammals are known for their outstanding agility underwater (Videler [1]), hence offering a novel paradigm for man-made vehicles, which could provide new concepts and technology to significantly enhance their agility underwater. In addition, the use of flapping foils is presently under consideration as a means of improving AUV maneuverability—concurrently with either fully providing propulsion, or assisting propulsion. Such foils can be designed biomimetically to emulate the performance of the fins and tails of live fish.

The rhythmic, oscillatory motion of fish body and fins results from an "impedance matching" between the dynamics of the actively controlled musculature and the fluid loads. This is a classical fluid-structure interaction problem that requires detailed understanding of the control laws employed by fish, the mechanical and material properties of the actuating muscles and the body of the fish, as well as the fluid mechanics of the flow around the body. Observations and studies of fish provide information on the body properties, while fluid mechanics studies provide insight on basic flow mechanisms; the overall problem, however, is still intractable to solve by simulation at high Reynolds numbers. Conceptual advances are needed in order to simplify the problem of fish locomotion, and not only make it tractable, but also provide engineering information to build man-made vehicles. Indeed, such vehicles employ different actuation mechanisms and control laws from fish; hence, it is expected that the "impedance matching" will not be the same, since the actuation methods are different—although the flow mechanisms are the same.

Two fundamental questions then arise, whose answers would benefit applications:

- Is the motion of fish affected by the mechanical and material limitations of their own body and the control laws they employ, i.e., is the final motion nonoptimal as far as fluid mechanics are concerned, due to structural, material, and control-law limitations?
- How can we extract, using biomimetics, optimal flow mechanisms that can also apply to different actuation and control mechanisms?

One must take into account the fact that motion within heavy viscous liquids, such as water, carries a heavy penalty on the energy required for locomotion and maneuvering if the motion is not optimized. It would pay, therefore, at least for the fastest and most agile animals, to exhaust every possible way to optimize the fluid mechanics of their locomotion—at the expense of redesigning their structure and control procedures; to the extent, of course, allowed by the available materials. This must be achieved through optimization of body geometry and structure, as well as body actuation and control.

The procedure we follow in this review is to consider data from live fish and cetaceans, as well as data from engineered flapping foils and fishlike robots. These data are reduced in terms of basic nondimensional parameters, derived on the basis of fluid mechanics scaling laws. These are derived through a combination of theoretical, numerical, and experimental methods in order to optimize the power needed for propulsion, or the energy required for turning and fast starting. The degree to which data from live fish, optimized robots, and experimental apparatus are in accordance with, or deviate from, these flow-based laws allows one to understand the effect of structural limitations, and provide impetus for conducting further experiments in the laboratory, to explain apparent differences, or to explore the possibility of live fish employing different flow mechanisms.

A basic concept that has been employed to explain fish swimming is that flow control for locomotion and maneuvering is best achieved through precisely controlled generation and manipulation of large-scale vortices; hence, the dynamic properties of fish bodies and their fins, as well as those of marine biorobots are to a large extent determined by the mechanisms of *vorticity control*. Scaling laws can be derived, therefore, on the basis of devising nondimensional parameters characterizing vortical flow control, such as to maximize thrust or force production for a given energy

Transmitted by Associate Editor W. Shyy.

input. We also outline the effect of these laws on the state of the boundary layer of the fish or biorobot.

This review focuses on hydrodynamically based scaling laws applicable to fishlike swimming; as such, it is by no means exhaustive of the available literature on fish swimming.

2 Overview of the Literature

Data from live fish and cetaceans have provided detailed description of how these animals employ their flapping body and tail, as well as their fins, to produce propulsive and maneuvering forces [1,2]; and the resulting flow features and patterns [3–9].

Since foils are the basic means for force production in fish, the fluid mechanics of foils have been investigated with the goal of understanding the principles of this different paradigm of propulsion and maneuvering using theoretical and numerical techniques [10–24] and experimentally [25–29]. It was found that unsteady motion of a foil causes the shedding of vorticity from the trailing and side edges and tips of the foil, and possibly from the leading edge as well. Distinct, stable patterns of large-scale vorticity have been discovered through visualization [28,30–38]. The number of large-scale vortices formed per cycle varies with the amplitude and frequency of the motion and the shape of the kinematics employed [28,33]. In Triantafyllou et al. [39,40], a stability analysis of the time-averaged jetlike flow behind thrust-producing flapping foils was performed; it was found that there are specific nondimensional frequencies that are optimal for energy minimization. Data from flapping foils and swimming fish and cetaceans show that they operate at nondimensional frequencies close to the theoretical values for optimal efficiency [41–46]. Freymuth [34] conducted experiments on a heaving and pitching NACA 0015 foil at Reynolds numbers from 5,200 to 12,000; he associates high values of the lift coefficient with the formation of a leading-edge vortex (dynamic stall vortex), which is shed and then amalgamated with trailing-edge vorticity. The mechanisms of leading-edge vortex formation have been investigated by Reynolds and Carr [47]. McCroskey [48] provides an extensive review of the effects of unsteady flow mechanisms on foils, including dynamic stall vortex formation.

Unsteady vortical patterns play a crucial role in the flight of insects, as reported by Maxworthy [49], Ellington [50,51], Freymuth [36], and Dickinson [52,53]. The mechanisms causing a large increase in the unsteady lift are, in the nomenclature of [53]: (i) delayed stall, (ii) rotational circulation in the form of an unsteady Magnus effect, and (iii) wake capture. Studies in [52,54] have further probed the effect of fin rotation. Ellington [50] and Maresca et al. [55] show a significant delay in stall caused by unsteady effects. Ohmi et al. [56,57] studied a translating and harmonically pitching foil with mean incidence angle of 15 or 30 deg and at Reynolds number from 1,500 to 10,000. They find that the forming vortical structures depend on the relative importance of the translational and rotational motion. When the rotational motion dominates, the governing parameter is the product of the reduced frequency and the amplitude-to-chord ratio—this product is proportional to the Strouhal number. Anderson et al. [28] experimentally studied a harmonically flapping (heaving and pitching) two-dimensional foil, and classified its vortical structures in terms of the following parameters: (i) maximum angle of attack, (ii) nondimensional frequency of oscillation (Strouhal number), and (iii) heave-to-chord ratio. Optimal propulsive performance was associated with moderately large angle of attack, formation of two vortices per cycle in the wake, and the development of small to moderate leading-edge vortices.

The three-dimensional (3D) vortical structure behind a finite aspect ratio rectangular flapping foil was visualized by Freymuth [37], Hart et al. [58], and Ellenrieder et al. [24], showing that leading-edge, trailing-edge, and shed vortices are all interconnected among themselves and with the foil.

Very few data exist for maneuvering foils and fish [6,59]. Similarly, very little is known about the cavitation properties of flapping foils; cavitation inception was found to depend on the reduced frequency and amplitude of oscillation [58].

3 A Review of Scaling Laws

3.1 Steadily Oscillating Foils for Propulsion. Propulsive, harmonically oscillating foils, under steady-state conditions, form a wake whose time-averaged form is that of a jet, as the momentum theorem also requires, in order to produce thrust. A jet flow is characterized by shear layers, i.e., continuous shedding of vorticity. Taking a different view, the foil sheds unsteady vorticity as it oscillates and translates forward; this vorticity organizes to form large-scale patterns, which are compatible with a jetlike time-averaged flow. A "reverse Kármán street," i.e., a double row of vortices in a staggered configuration producing a jet flow, is one of many such possible patterns, as pointed out in early work by Kármán and Sears, and predicted in the works by Lighthill [10] and Wu [11]. Recent work has shown that the reverse Kármán street holds certain optimality qualities, i.e., for a given thrust it requires the least energy. In two-dimensional (2D) foils, as well as high aspect ratio foils and foils with end plates, a planar cut in the wake shows that two vortices per cycle is the optimal pattern, i.e., a reverse Kármán street; more than two vortices may form, symmetrically or asymmetrically [33,60], resulting in a decrease of thrust generation or propulsive performance [28,33]. Foils performing only a pitch motion [33], foils performing a heave motion [38], and heaving and pitching foils [25,28] may produce reverse Kármán streets under proper conditions. Multiple vortices may form outside the proper parametric range; also, instabilities may form. For example, for large Strouhal number, foils under heave motion develop a vortex street at an angle with respect to the oncoming velocity, resulting in steady lift as well as thrust. The instability may develop on either side of the foil, depending on the starting conditions, while switching from side to side is possible due to external forcing [38,61].

The shedding and subsequent organization of vorticity is an essential mechanism for propulsion, and the stable coexistence of the unsteady vortical patterns with a jetlike time-averaged flow is a characteristic of optimally operating foils. Since the time-averaged flow is unstable to small perturbations in the form of a highly tuned amplifier, such dynamic equilibrium would require that the unsteady patterns formed behind the foil have frequency and wavelength close to that of the most unstable mode of the time-averaged flow ([39,40]). An analysis of jetlike profiles measured behind flapping foils shows that the optimal nondimensional frequency has a value in the range of 0.25 to 0.35. The reduced frequency parameter in flapping foils was named the *Strouhal number* in [39,40] to bring attention to the similarities between the vortical flows behind bluff bodies (where the name originated after Strouhal's pioneering studies [62]) and flapping foils. There is also, however, a basic difference between the two types of flow, since the Strouhal number is a "natural frequency" of the bluff body wakes, which are characterized (locally) as absolutely unstable flows. Jet flows behind flapping foils are also unstable, but have no such "natural frequency," because they are convectively unstable [40], spatially amplifying an imposed excitation. Hence, a more suitable name would be the *reduced frequency*, as also used in bluff bodies when considering forced oscillation flows; nonetheless, the Strouhal number has been established, and is widely used now in the literature, defined as the ratio of the product of the frequency times the width of the jet formed behind the foil, divided by the average flow in the wake

$$\mathrm{St} = fA/U_m \tag{1}$$

The width of the jet A and the average velocity in the jet U_m are difficult to calculate a priori since the width of the wake is typically not available, while the average flow velocity in the wake (accounting for the increase in velocity within the jetlike flow) depends on the thrust level and the kinematics of the flow, and is also unavailable. As a result, A is approximated by the excursion of the trailing edge of the foil A_t; and instead of using an average jet speed, the forward speed U is employed:

$$\mathrm{St} = fA_t/U \tag{2}$$

There are limitations to this definition: When the foil is heavily loaded, i.e., producing a large thrust coefficient, the average jet velocity will be substantially different from the forward velocity U; this is especially true under steady hovering conditions, $U=0$, when the Strouhal number in Eq. (2) is undefined; Eq. (1) can still be used, but U_m has to be measured or calculated. Also, the width of the wake may be different from the excursion of the foil. For pitching foils, the excursion of the foil varies significantly along the chord; we employ the maximum excursion of the trailing edge. The basic fact is that *the Strouhal number is a wake parameter*, and only indirectly a foil parameter; definition (2) should be used with this clarification in mind. In [23], the efficiency of a two-dimensional flapping foil was studied as a function of the frequency; it was shown that for moderate Strouhal numbers, optimal efficiency is obtained close to the frequency of maximum spatial amplification predicted by the average jet flow, i.e., in agreement with optimal Strouhal number scaling.

The Strouhal number provides a basic scaling law for the hydrodynamics of flapping foils under steady-state conditions. Returning to the original question of the effect of the impedance matching between structure and flow, it appears from the analysis of fish data that the Strouhal scaling law is a basic governing parameter, i.e., there does not appear to be a significant deviation from the law due to the elastic properties of the actuating muscles or the body. In [43], several observational data from marine mammals are presented and analyzed. Most reduced data fall in the range of St between the values of 0.20 and 0.40. Agreement is good, since one must take into account the fact that the tails of fish operate within their own body's wake; interactions between oncoming body-generated vorticity and caudal fin vortices alters the average jet flow [63]. We may conclude that the structural parameters are capable of conforming—and have in fact conformed—to this hydrodynamic requirement.

There are special requirements for the fish structure, its material properties, and the actuation and control mechanisms employed for the fish body and fin motion. A central requirement, for example, is the recovery of the inertia energy during a complete cycle of motion. Indeed, the unsteady rhythmic motion of fish requires, for efficiency, to be able to recover the inertia energy within a cycle, store it as potential energy, and then use it again. This can be achieved only if the combination of the virtual body mass (accounting for added mass) and the body elastic stiffness provides a natural frequency very close to the frequency of operation. Since it is known that the amplitude of motion of the fish tail does not vary substantially [1], the frequency of tail flapping must vary linearly with speed, at least in the high-performance range; this would require a dynamic control of body elasticity in order to commensurately change the natural frequency of the body and, hence, recover energy efficiently (see Fig. 1).

The requirement for energy recovery places similar restrictions on man-made flapping foils: The amplitude of motion of the foil is likely to remain constant—as in the case of fish; the reason for this is hydrodynamic efficiency. It has been found that in 2D foils, a heave motion with amplitude approximately equal to one chord length is associated with the largest efficiency. Hence, frequency must be varied linearly with the speed of operation in order to preserve the optimal Strouhal value. This would imply a dynamically controlled natural frequency of the structure in order to have matching between Strouhal frequency and structural natural frequency.

There are several other parameters in steady propulsion. Taking the case of a heaving and pitching foil with a bias angle, there are six physical parameters: the forward speed U, the heave amplitude h_o, pitch amplitude θ, bias pitch amplitude θ_b, frequency f, and

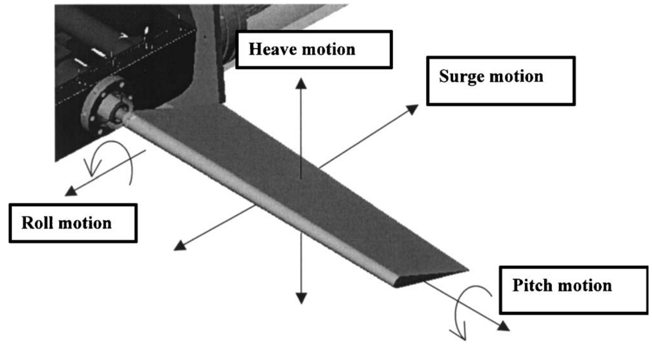

Fig. 1 Motion definitions: Surge—rowing motion along the *x*-axis, heave—linear up-and-down motion about the *z*-axis, and roll—motion causing equivalent heave motion at any specific spanwise location about the *x*-axis, pitch—motion about the *y*-axis

phase angle between heave and pitch ψ. In addition to the Strouhal number St, there are five other nondimensional quantities: the heave to chord ratio h/c, maximum angle of attack α_o, pitch bias angle θ_b, the phase angle ψ, and the Reynolds number Uc/ν, where ν is the kinematic viscosity. The maximum angle of attack, as shown in Fig. 2, is defined as the maximum value over a period of oscillation of the angle of attack $\alpha(t)$

$$\tan[\alpha(t) + \theta(t)] = (\mathrm{d}h/\mathrm{d}t)/U \tag{3}$$

where $\theta(t)$ denotes the pitch motion and $y(t)$ the heave motion

$$h(t) = h_o \sin(2\pi ft) \tag{4}$$

$$\theta(t) = \theta_o \sin(2\pi ft + \psi) \tag{5}$$

Some of these parameters lie in narrow ranges; detailed hydrodynamic data on flapping foils show that the maximum efficiency is achieved for h/c between 0.75 and 1.0, a very narrow range.

Also, the phase angle between heave and pitch has a moderate effect on efficiency, with a nominal value of $\psi=90$ deg providing acceptably good efficiency values. The bias angle is needed only when steady transverse forces are to be produced; the bias angle depends on the required magnitude of the steady force. Foils oscillating around a steady pitch angle θ_b produce asymmetric wakes and, hence, generate a steady lift force [36,37]. The wake can be inclined with respect to the oncoming flow, and the vortices on one side of the wake have larger circulation than on the other, while the number of vortices on one side of the wake may be larger than on the other side. In a hovering mode, when $U=0$,

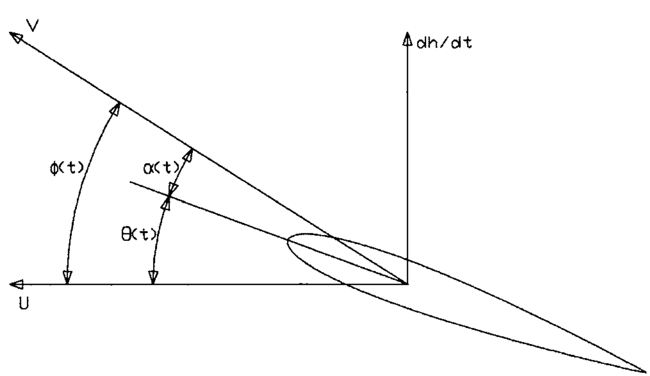

Fig. 2 Angle-of-attack definition for a two-dimensional foil traveling at constant forward speed *U* and oscillating in a heave-and-pitch motion

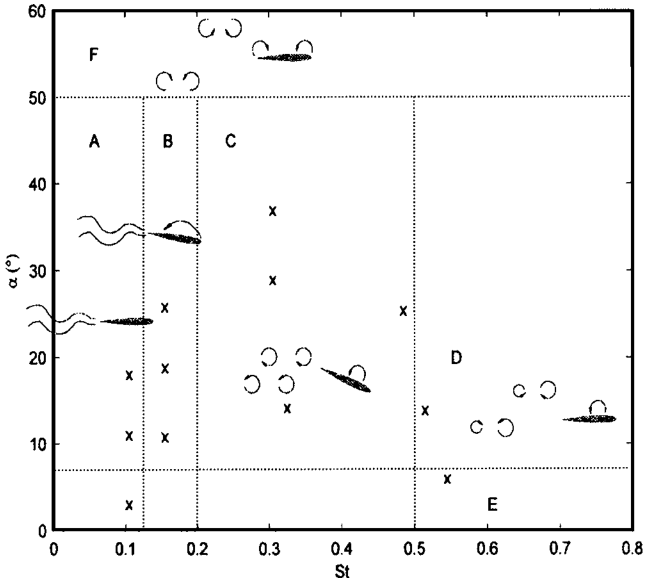

Fig. 3 Wake patterns as functions of the Strouhal number and maximum angle of attack for $h_o/c=1$. Points mark the experiments conducted by Anderson et al. [28].

a bias angle allows to vector arbitrarily the steady force produced [37].

The maximum angle of attack has a significant effect on efficiency and on the form of the vortical patterns in the wake. Figure 3 [4,28] provides a synoptic view of the visualization data on the flow around a two-dimensional flapping foil as a function of the two most significant parameters, the maximum angle of attack and the Strouhal number. We distinguish the following regions: In the regions of low Strouhal number, A and B ($St<0.2$), the wake does not roll up into discrete vortices—instead, it retains a wavelike structure; in region B, a very weak leading-edge vortex appears for $a_o>30$ deg, but the wake retains its wavy form. For moderate St and angles of attack (region C), contained between the parametric values of 7 deg$<a_o<$50 deg and $0.2<St<0.5$, a reverse Kármán street forms, consisting of two vortices per cycle. A leading-edge vortex forms for angles of attack larger than about 10 deg, which increases in strength with increasing angle of attack, but is amalgamated with a trailing-edge vortex—hence, the wake always forms two vortices per cycle. For large St ($St>0.5$) and for angles of attack smaller than 5 deg (region E), the wake does not form any distinct patterns. For larger angles of attack (region D), leading-edge vortices form that pair with trailing-edge vortices—the wake forms four vortices per cycle. For all St and large angles of attack, larger than about 50 deg, a pistonlike mode appears, where leading- and trailing-edge vortices form simultaneously and roll up in the wake to form four vortices per cycle (region F).

The data shown are for $h/c=1$; for other values of h/c, qualitatively similar regions are found, although the specific parametric regions depend on h/c.

The presence of a leading-edge vortex affects efficiency; a mildly strong leading edge vortex may increase propulsive performance [28]. The development of a leading-edge vortex depends on the Strouhal number, but is dominated by the angle of attack; the subsequent interaction with trailing-edge vorticity depends on Strouhal number. In region C, for St in the range between 0.2 and 0.5, strong thrust develops from a reverse Kármán street, accompanied by up to a moderately strong leading-edge vortex; this is a region of high propulsive efficiency. In region D, for St larger than 0.5, strong thrust develops accompanied by the formation of four vortices per cycle, consisting of two pairs of counterrotating vortices; in each pair, the two vortices have, in general, different circulations. In regions A and B, low or negative thrust develops, associated with a wavy wake with no distinct vortex formation, while the leading-edge vortex is also very weak. In region E, for very small angles of attack, very small or negative thrust develops.

Although, in most studies, sinusoidal kinematics are employed for flapping foils, it is important to consider whether such a sinusoidal motion is optimal in terms of propulsive efficiency. Koochesfahani [33] experimentally studied various deviations from a purely harmonic pitching oscillation of a foil. He found that, within the optimal Strouhal number range, the purely sinusoidal motion produces a clean reverse Kármán street (two vortices per cycle); whereas any other motion produces additional vortices per cycle. Since a reverse Kármán street is found to require minimal energy for a given thrust level, this indicates that a purely oscillatory pitching motion is indeed optimal. For a heaving and pitching foil, however, Hover et al. [64] found a different result: The optimal kinematics, in terms of providing maximum propulsive efficiency, are not purely sinusoidal heave and pitch motions; instead, maximum efficiency was obtained when a multifrequency heave motion was used that, in combination with a sinusoidal pitch motion, produced a purely harmonic angle of attack. The explanation for this is evident from Eq. (3), where it is found that the angle of attack contains higher harmonics for a purely harmonic heave motion (due to the inverse tangent function). When the heave motion is chosen to contain higher harmonics in such a way as to cancel the high harmonics in the angle of attack, then the wake produces two vortices per cylce, and the highest efficiency is obtained. *This means that the angle of attack, as defined in (3), is the major controlling parameter in vortex pattern formation, hence, affecting efficiency*.

3.2 Three-Dimensional Effects in Flapping Foils. As found in [65], the performance of oscillating *delta* wings does not depend on the reduced frequency (or equivalently, the Strouhal number) until large angles of attack are reached. The flow mechanisms are different in the case of delta wings because the dominant vortices ("leading-edge" vortices) forming on the sides of the delta wing remain attached and are convected downstream through a helical fluid motion. Hence, the wake is drastically different from in a rectangular, high-aspect-ratio wing, and there is no characteristic time scale for these leading-edge vortices.

In *rectangular* three-dimensional flapping foils, the aspect ratio has an effect on the vortical patterns and, hence, potentially on the scaling laws. Since the vortical patterns must connect with each other and with the foil producing them, the dynamics of the large-scale vortical patterns are influenced by the span-to-vortex spacing ratio. Lighthill [10] sketched an idealized chain of alternately inclined, with respect to the direction of motion, interconnected vorticity rings; this has been shown experimentally to adequately represent the flow behind oscillating fish fins [7–9]. Detailed flow visualization in flapping foils provides a more complex picture: The vortical patterns form closed-ring loops; the vorticity of each loop connects all the way back to the foil [35,37,58] in the same way that Kármán vortices formed behind bluff bodies interconnect with themselves and to the body. Overall, the three-dimensional effect of the aspect ratio on the forces is reduced as frequency increases because the tip vortices are of alternating sign, hence, the induced velocities are significantly reduced. As Freymuth [37] remarks, the overall picture in three-dimensional wings is a "curious mixture of two-dimensional and three-dimensional vortex developments…." This was confirmed by Karpouzian et al. [15], Cheng et al. [66], Martin [67], Martin et al. [68], and Dickinson et al. [53] for flying animals.

Freymuth [37] shows pictures for rectangular, low aspect ratio foils under high angle of attack, where both leading- and trailing-edge vorticity form; the trailing-edge vortices form rings connecting to the foil edges with alternating sign tip vortices, while the leading-edge vortices form separate rings through shedding. Ellenrieder et al. [24], in experiments at Reynolds number 160, and

Guglielmini [61], using direct numerical simulation (DNS) at the same Reynolds number, explored the vortical structure of flapping foils with aspect ratio 3: Vortical structures have the expected structure of interconnected rings at moderate Strouhal numbers and angles of attack, with the leading-edge vortices contributing significantly to the vortex formation. The rings may resemble "irregular pancakes," or may contain additional, secondary loops [24]. For high St, the flow develops into two diverging concatenated chains of rings [61].

Maxworthy [49] proposed that, in nonrectangular wings, leading-edge vortices are helical vortices that connect to the tip vortices. Numerical simulations of the wing of a hovering insect [13,20] show a similar structure. This is a different vorticity shedding mechanism than in two-dimensional foils, because a helical vortex continuously convects downstream.

Scherer [25] reports efficiency in rectangular, moderate aspect ratio wings of up to 70%; his Strouhal numbers were kept moderately low and did not reach the regions where maximal efficiency is anticipated. Lai et al. [27] report efficiencies up to about 75% for a flapping rectangular NACA 16-012 foil with aspect ratio 4. DeLaurier and Harris [26] report efficiencies in the range of 18 to 50% for a rectangular NACA 0012 flapping foil with aspect ratio 4, oscillating with heave amplitude equal to 0.625 chords, at Reynolds number 30,000.

Kato [69–71] has considered the forces generated by a foil hinged at a single point, with aspect ratio of order 1—the aspect ratio found typically in the pectoral fins of fishes [1]. The fins performed three types of motion: (i) rowing, i.e., forward-backward motion, or surge in the notation of Fig. 1; (ii) feathering, i.e., a twisting (or pitching) motion about the axis of the fin; and (iii) flapping motion, i.e., rolling motion about the root attachment of the fin transversely to the flow, when a steady stream exists. The propulsive efficiency of feathering or flapping foils, which is lift based, is larger than the efficiency of drag-based rowing foils, in agreement with Walker and Westneat [72], who show a maximum efficiency of 10% for drag-based propulsion, contrasted with about 60% maximum efficiency for lift-based propulsion. Rowing is better suited for still water (zero forward motion) force generation, providing potentially better maneuverability at such speeds. A nonsinusoidal feathering motion combined with a sinusoidal rowing motion produces thrust accompanied by smaller transverse forces. Maximum efficiencies of the order of 45% are reported for the lift-based mode of propulsion by Kato [70,71].

3.3 Multiple Foils and Foils Interacting With Bodies. When two or more foils operate side by side (such as employed by penguins [73]), or foils operate near a wall or are attached to a vehicle, there are important interaction effects taking place. In [74], a streamlined vehicle equipped with two flapping foils in close proximity was studied. Force and efficiency measurements, as well as flow visualization, show strong interaction effects that require additional parameters compared to single foils. Flow visualization in two side-by-side foils shows that when they oscillate very close to each other, a strong drag wakelike flow develops between the foils causing efficiency deterioration. The wakes of two flapping foils may develop the following forms [75]:

1. The two wakes can collapse into a single wake.
2. The wakes interact strongly, forming two jets divided by a backflow region, which can deteriorate performance seriously.
3. The wakes are well separated, providing good thrust performance.

When foils flap against a body, or against a second foil, the conditions of the Weis-Fogh mechanism apply. Large forces are produced, but these include large drag forces, while the resulting vortical patterns are different from those for single foils. In Tsutahara and Kimura [76], the Weihs-Fogh mechanism is used to produce thrust for ship propulsion. The mechanism was first associated with high lift production in insect flight by Weis-Fogh [77]: Two identical 3D wings initially rest against each other. The first stage of motion begins with a rotational motion whereby both wings rotate away from each other, while hinged at one of their edges. The second stage consists of the foils detaching completely, when large bound circulation develops in the foils (of opposite sign in each wing), resulting in high lift force production. Subsequently, a reverse rotational motion brings the foils together, and so on (Maxworthy [49]). In [78], two rectangular plates with aspect ratio 1.8 were used up to Reynolds number 300,000. The efficiency was up to 58% for angular amplitude of 15 deg, lower for other conditions.

In [74,78], two foils flapping against a middle flat plate were employed. Efficiencies up to 30% are reported, while the vortical patterns form a rapidly expanding wake.

3.4 Maneuvering and Fast-Starting Foils. Maneuvering is an essential function in fish with important lessons for technological applications (Webb [79,80]; fast-starting fish exhibit outstanding performance [81,82]. In maneuvering and fast starting, a foil must also provide either a steady transverse force or a transient, high-magnitude force. The generation of unsteady vortical patterns is at the root of the performance of maneuvering foils, hence there are similarities with steadily flapping foils. The details differ, however, and hence the physical mechanisms and properties have differences as well. Published data include foils performing a transient motion [29,68,83]; steadily flapping foils around a bias angle, in order to develop steady lift forces [29,56,57,84]; and foils in combination of rowing, plunging and feathering motions, together with bias angles to develop nonsinusoidally varying lift [55,69,70,85,86]. Hertel [87] and Ahlborn et al. [59] showed that a flapping foil develops a pair (or pairs) of interconnected vortices (which appear like rings in a three-dimensional view) when starting from a position of rest and performing a complete cycle of heave or pitch motion. Drucker and Lauder [7,8] show the formation of sequences of inclined, interconnected ringlike structures in the wake of flapping pectoral fins of live fish. Ohmi et al. [56] report that the bias angle in a pitching foil plays a significant role in determining the flow patterns up to a threshold nondimensional frequency, proportional to the Strouhal number. In [29,57], a bias angle is used to produce steady lift in unsteadily flapping foils. Significant steady and unsteady lift, higher by up to an order of magnitude than under steady conditions, can be produced. The moderate aspect ratio, three-dimensional foil in Martin et al. [68] produced steady and unsteady lift forces comparable to those experienced by the two-dimensional foil employed by Read and Hover [84]. This demonstrates once more that end effects are less important in unsteady foils than steady foils, in accordance with the findings in [14,29,52].

As shown in Fig. 4, a three-dimensional foil performing two angular harmonic motions about a single hinge point, one transverse to the oncoming flow and one about its long axis (roll motion as defined in Fig. 1), can develop steady lift coefficients of order three, much higher than for steadily translating foils, while it can also develop thrust.

In a fast-starting foil, the specific kinematics employed can have a significant effect on the resulting forces. Figure 5 shows the specific kinematics employed in a 2D foil, wherein the motion starts with a maximum heave and pitch motion, undergoes a complete harmonic cycle, and returns to its original position. The resulting thrust and lift forces (Fig. 6) undergo large variations, which are determined by the heave and pitch acceleration (added masslike forces) and heave and pitch velocity; the velocity-dependent terms are dominated by the shedding of large-scale vortices, which have their own time constants [89,90], governed by laws analogous to the Strouhal laws of steadily flapping foils [39,40] and the impulsive vortex-ring formation laws [91–93].

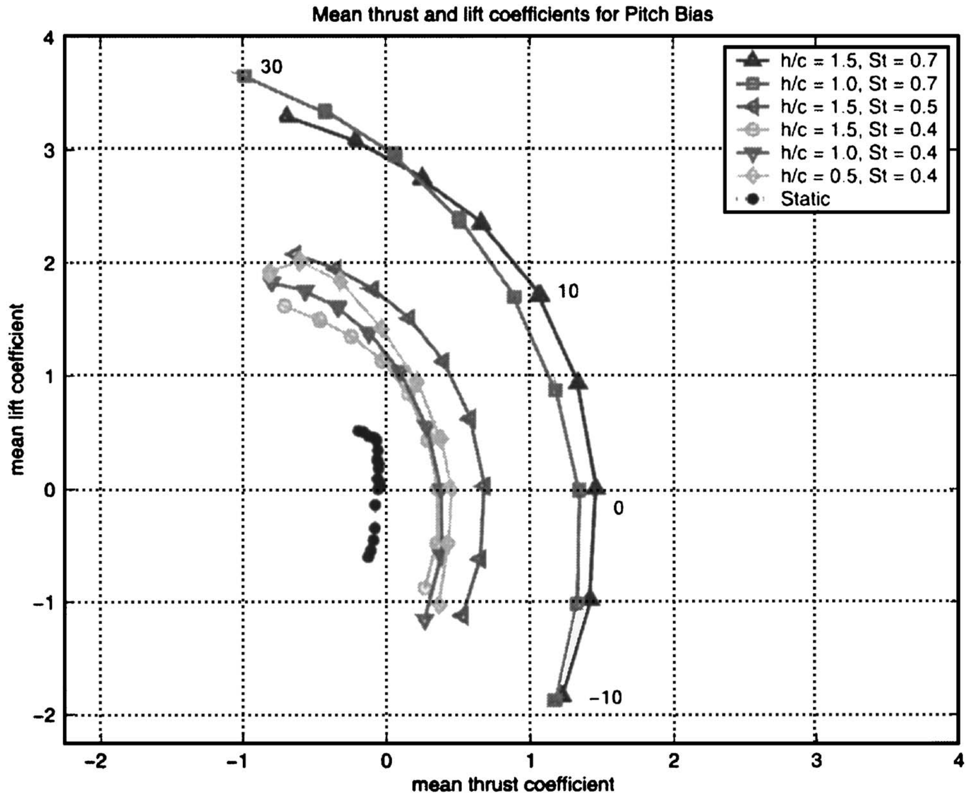

Fig. 4 Mean lift and mean thrust coefficient of a three-dimensional pitching and rolling foil, for bias angle from −10 to 30 deg. Equivalent heave is defined at 0.75 of the radius; the curve marked Static provides the data for a steadily towed foil at an angle of attack [88].

3.5 The Interaction of Foils With Oncoming, Externally Generated Vorticity. Foils operating within unsteady flows, such as turbulent streams, ocean waves, or within the wakes of upstream objects, can, under favorable conditions, extract energy from the oncoming flow. There are two paradigms of foil-unsteady flow interaction: a foil flapping within waves ([94]), and a foil interacting with oncoming vortices. For the latter case, reports are provided in Sparenberg and Wiersma [95], Koochesfahani and Dimotakis [96], Gopalkrishnan et al. [97], Streitlien et al. [18], and Beal et al. [98]. Gopalkrishnan et al. [97] identified three modes of foil-vortex interaction:

1. Oncoming vortices interact destructively with trailing-edge foil vortices of the opposite sign, forming a street of weak vortices (destructive mode); propulsive efficiency increases.
2. Oncoming vortices merge with same-sign foil-generated

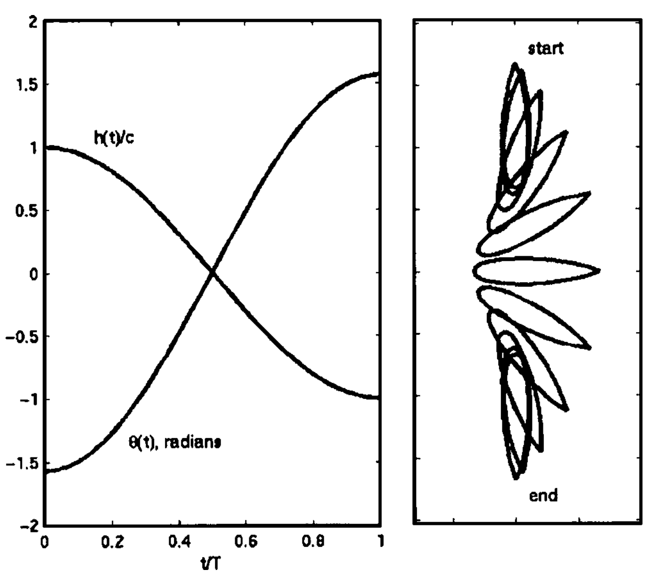

Fig. 5 Kinematics of fast-starting two-dimensional foil in heave and pitch motion [29]

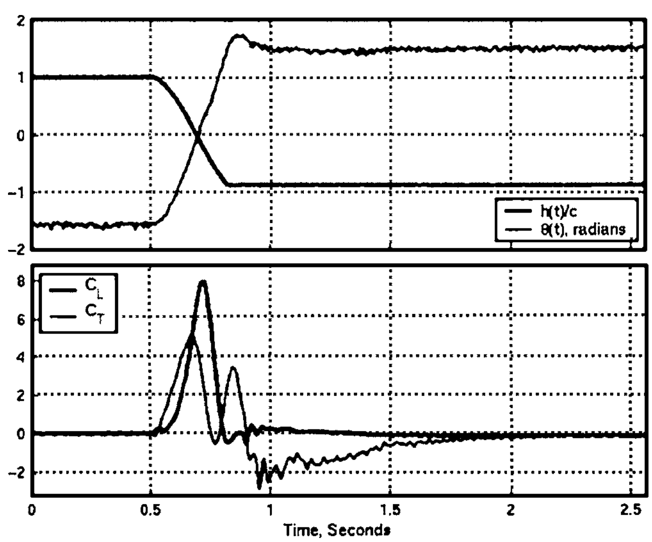

Fig. 6 Heave and pitch velocity (upper figure) and resulting thrust and lift forces (lower figure), as functions of time for the kinematics shown in Fig. 6 [29]

vortices (constructive mode); reduced efficiency results.

3. Upstream vortices pair with opposite-sign foil-generated vortices (pairing mode), with varying effect on efficiency.

Anderson [4] showed that leading-edge vorticity can interact earlier with oncoming vortices than trailing vortices. The resulting patterns resemble, overall, the three major patterns of [97], although differing in several details of the flow, especially close to the foil, hence affecting performance.

In order for a foil to extract energy from oncoming unsteady patterns, two conditions must hold:

1. The foil must flap at a frequency close to the frequency of the oncoming vortices.
2. The size of the oncoming vortices must be comparable to the foil chord.

Hence, any sensing and control scheme employing a foil must satisfy these two basic conditions. Observations with live fish swimming behind bluff cylinders confirm these laws [99,100], using the fish length as the proper length scale.

3.6 The Influence of Reynolds Number on Foil Performance. Fishes span a wide range of length L and swimming speed U, and hence of Reynolds number based on fish length, $\mathrm{Re}_L = Ul/\nu$, where ν the water kinematic viscosity—from 10^2 to 10^8. The tail has an average chord length of the order of 10% of the length L; hence, the Reynolds number Re, based on the average tail chord length c, is in the range from 10^1 to 10^7, while the majority of experimental and computational data is obtained for relatively low Re. The effect of Re is to alter the boundary layer of the foil, especially in the transition between laminar and turbulent flow, and hence affect the formation of vortices.

One basic question is on the value of the drag of a flapping foil, which cannot be measured directly since drag and thrust are inseparably interconnected. The drag coefficient of a steadily towed foil c_D is defined as

$$c_D = D/[(1/2)\rho U^2 A_f] \tag{6}$$

where D is the measured drag force (frictional plus form drag), ρ is the density of water, A_f is the foil area (average chord times average span), and U is the towing velocity.

In the case of a flapping foil, the measured axial force is the total force, the sum of drag and thrust components. A way to estimate the drag coefficient of a flapping foil is to compare the experimentally measured thrust and efficiency of a flapping foil with the thrust and efficiency predicted by ideal flow (inviscid) theory. Figures 7 and 8 provide the thrust and power coefficients c_t and c_p, respectively, as functions of the Strouhal number, defined as $\mathrm{St}=2hf/U$, where h is the heave amplitude; for constant maximum angle of attack (15 deg) and heave-to-chord ratio (0.75) for an NACA0015 foil.

The coefficients are defined as

$$c_t = T/[(1/2)\rho U^2 A_f] \tag{7}$$

$$c_p = P/[(1/2)\rho U^3 A_f] \tag{8}$$

where T is the average (net) thrust, P is the time-averaged power required, and the other quantities are defined as in Eq. (6).

The experimental data, obtained at Re=37,000, are compared against linear inviscid theory [11,10] and nonlinear inviscid theory [17]; the theory can be viewed as an "infinite Reynolds number limit." It is clearly seen that the power coefficient is very close to the theory across the entire St range, while the thrust coefficient of the experiment is lower than the theoretical one, by almost a constant value within a relatively wide range. An average value of c_d=0.063 can be inferred from Fig. 7 across the St range; this is the average distance between experiment and nonlinear theory, which can be thought of as the unsteady drag coefficient of the foil. Measurements of the drag coefficient for a nonflapping foil, towed at zero angle of attack, provide a value of c_d=0.068 for Re=30,000 and c_d=0.05 for Re=40,000. For comparison, Hoerner [101] provides a value of c_d=0.043 for a 13% thick foil and c_d=0.06 for 20% thick foil, both values at Re=40,000. These values of the drag coefficient under steady conditions are very close to the value of the unsteady drag coefficient.

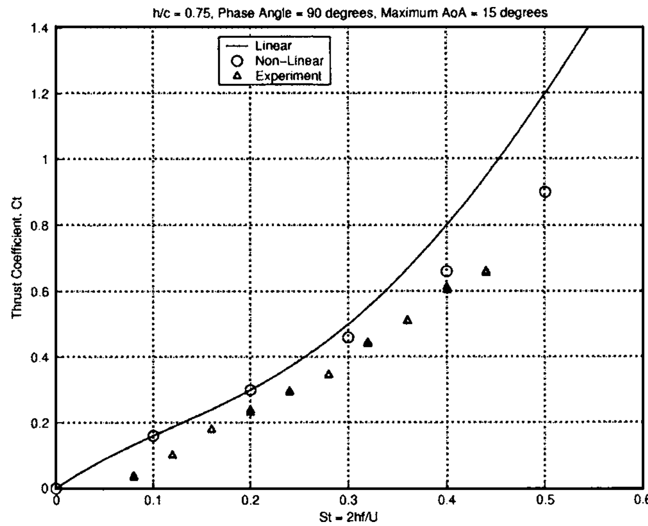

Fig. 7 Thrust coefficient as function of Strouhal number for 15 deg angle of attack and h/c=0.75. Triangles denote experimental data, solid line linear inviscid theory, circles nonlinear inviscid theory [28]

In conclusion, the principal effect of the Reynolds number, based on chord length, appears to be a decrease in the drag coefficient as Re increases—at least for subcritical Reynolds numbers, i.e., below Re approximately equal to 5×10^5, for which we have available experimental data. The change in the drag coefficient of the flapping foil, as the Reynolds number changes, appears to be quantitatively close to the change in the drag coefficient of a nonflapping foil. This also means that there is no significant drag increase in a flapping foil due to its unsteady motions, at least for St values of <0.5. Efficiency, as a result, increases as Reynolds number increases, when all other parameters are kept the same.

Motani [45] uses an empirical power law connecting the power required for fish propulsion to the Reynolds number; then he com-

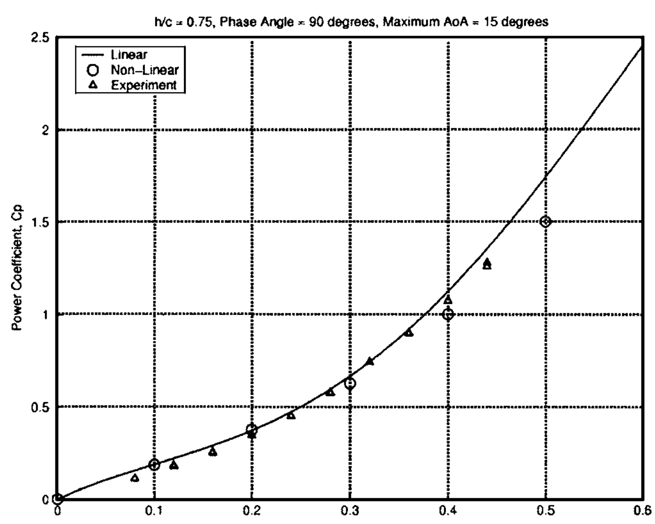

Fig. 8 Power coefficient as function of Strouhal number for 15 deg angle of attack and h/c=0.75. For symbols, see Fig. 7.

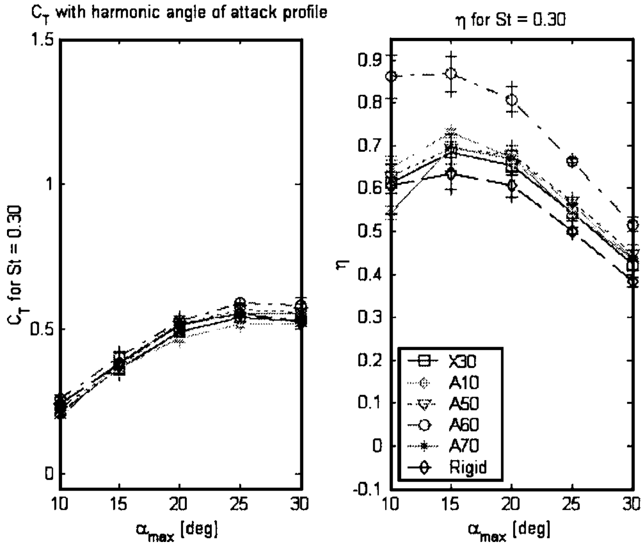

Fig. 9 Thrust coefficient (left) and propulsive efficiency (right) as functions of the maximum angle of attack for several foils of varying flexibility, classified according to Shore toughness: X30 is most flexible, A10 to A70 denotes increasing stiffness. Solid line is for rigid foil, while vertical bars express experimental accuracy [104].

bines the power law with the Strouhal number being in the range of 0.25 to 0.35 to arrive at a predictive law for optimal frequency and locomotion speed, which is in agreement with observational data.

3.7 Scaling Effects of Flexing Stiffness of Foils. Fish fins are known to be flexible, in the spanwise and chordwise directions; some fish have very flexible fins, others have stiffer fins, although fin flexibility appears to be largely passive. Theoretical, inviscid calculations on the effect of chordwise flexibility predict a decrease in thrust coefficient accompanied by an increase in propulsive efficiency, compared with a rigid foil [102]. Recent experimental work [103,104] shows that chordwise flexibility can improve efficiency substantially relative to a stiff foil, up to 38%, accompanied by only a small decrease in the thrust coefficient. Figure 9 shows the thrust coefficient and the propulsive efficiency as function of the maximum angle of attack for several two-dimensional foils of varying chordwise flexibility, classified according to Shore toughness. The Strouhal number is St=0.30, the heave-to-chord ratio is equal to 1, the phase between heave and pitch is 90 deg, and the Reynolds number Re=37,000. As shown, the thrust coefficient varies little; the maximum efficiency, however, varies substantially from a value of 0.62 for the rigid foil to a value of 0.86 for a foil with optimum flexibility.

Since the propulsive foil efficiency can vary by more than 38%, reaching values in excess of 0.80, flexibility appears to be a prime parameter in designing efficient flapping foils. As shown in Prempraneerach et al. [104], the prime scaling flexibility parameter is the following ratio, Δ:

$$\Delta = (45/2)(\rho c_L U^2/E)(c/h)^3 \tag{9}$$

where ρ is the density of water, c_L is the lift coefficient (which is typically of order 1), U is the speed of operation, E is the equivalent Young's modulus, c is the chord, and h is the average thickness of the foil. The optimal value is found around $\Delta = 1/3$.

Spanwise flexibility is considered theoretically in [105,106]. Actively controlled flexibility is proposed in [107] as a means employed by fish to increase their efficiency.

Spanwise fin flexibility also plays a significant role on the forces, power required, and efficiency of propulsion, as observations and studies in animals show [107–111]. References [107,108] suggest that actively controlled spanwise flexibility is employed by animals.

3.8 Scaling Laws in Fish-like Swimming. Fish employ a different paradigm of locomotion, involving large-amplitude flexing of their body. Biomimetically designed fishlike robots [112,113] demonstrate that different flow control mechanisms are involved in fishlike propulsion. The propulsive wake is characterized by the dynamic interaction of large-scale vortices arranged in a manner to efficiently induce a propulsive jet. As a result, based on hydrodynamic grounds, the frequency is expected to be dominated by a Strouhal-like law as outlined in the section on flapping foils. Measurements from live fish support this scaling [39,40,43,45,46].

Since the body wave flexure has the form of a traveling wave of increasing amplitude from head to tail, there are two additional characteristics to consider:

1. the wavelength λ of the traveling wave
2. the form of the amplitude envelope

The form of the amplitude envelope is controlled by the requirements to reduce backlash from the unsteady lateral motion of the body, and the need to reduce separation to the extent possible; as a result, the faster fish employ an amplitude envelope that restricts motion to the last half or one-third of the body length.

Theoretical arguments show that the phase speed c_p of the traveling wave must be larger than the forward speed U_o in order for the body to contribute to the thrust production [11]. As a result

$$C_p/U_o = f\lambda/U_o > 1 \tag{10}$$

Techet [114] and Techet et al. [115] showed that the turbulence intensity in the boundary layer of a robotic tuna like fish, as well as the boundary layer of a plate undergoing traveling wave motion within a stream of velocity U_o, is minimized anisotropically, but substantially, for all Reynolds numbers up to a value of 10^6 that was tested (see Fig. 10). Also, separation was found to be reduced significantly, as also reported in Taneda [116]. Turbulence intensity is reduced as c_p/U_o increases, reaching a minimum value for a value around $c_p/U_o = 1.2$; a flat minimum in the range of c_p/U_o between 1.1 and 1.5 is found. Beyond this range, turbulence intensity starts increasing again. At the phase speed of minimum turbulence intensity, separation appears to be completely eliminated. DNS calculations at Reynolds number up to 18,000 show that the total drag coefficient reaches a minimum value as well [117].

This requirement of $c_p/U_o = 1.2$ is in accord with the condition for thrust production by the body, which is $c_p/U_o > 1$. It places a much tighter range on the wavelength λ, which can now be directly estimated, once the frequency f_o is found on the basis of a Strouhal-like law, through the relation

$$f_o\lambda/U = 1.1 \text{ to } 1.5 \tag{11}$$

In [1], values of c_p/U_o are reported for two species: (i) for cod, it is found that c_p/U_o is in the range between 1.29 and 1.37; and (ii) for the saithe, a single measurement of 1.19 is reported. As with foils, the problem of fish swimming requires "impedance matching" between the structure and the fluid. The actuation of body flexing is one of the most complex flow-structure interaction problems because the integral of the side force must be as close to zero as possible and the effective drag must be minimized, while a thrust force equal to the body drag must be produced. Nonetheless, the Strouhal law appears to dominate the frequency of oscillation because the large-scale vortices play such a central role in the hydrodynamics of fish swimming.

4 Conclusions

Available scaling laws in aquatic locomotion and fishlike swimming have been reviewed, grouped as follows:

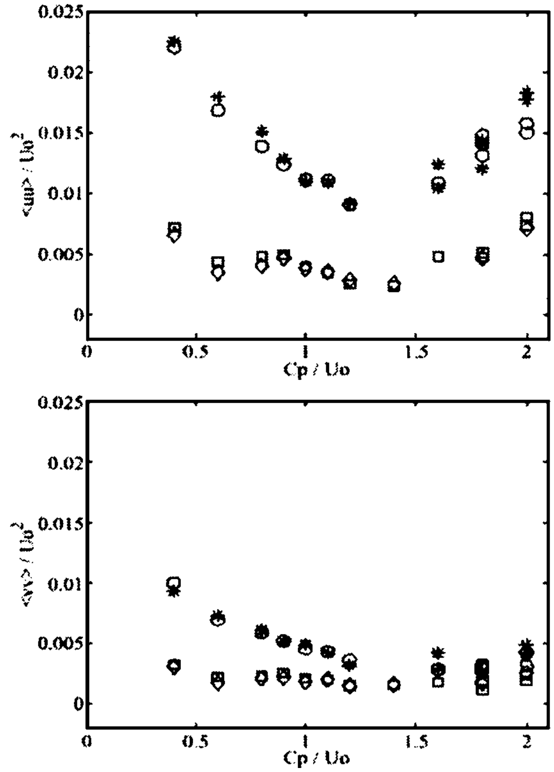

Fig. 10 Turbulence intensity in the axial direction (upper) and the transverse direction (lower graph) as functions of the phase velocity c_p for a two-dimensional flexible plate undergoing harmonic wave oscillation with a linearly tapered amplitude from leading to trailing edge [114].

1. Steadily flapping, high aspect ratio foils, used for propulsion: the Strouhal number, the amplitude of motion-to-chord ratio, and the maximum angle of attack are the dominant parameters because they affect the vertical patterns in the wake and, hence, thrust production and efficiency.
2. Three-dimensional effects in flapping foils: the aspect ratio and geometric shape (rectangular versus delta shape) of the foil—as for steadily towed foils—are the principal parameters for three-dimensional foils; in addition to the parameters applicable to high aspect ratio foils.
3. Multiple foils and foils interacting with bodies: vortical interactions among the wakes of multiple foils and interaction of shed vorticity with walls control foil interaction phenomena. Hence, the ratio of the transverse size of the foil wake compared to the principal distance to other foils and walls is the principal controlling parameter.
4. Maneuvering and fast-starting foils: the time to develop a full vortex ring is the principal parameter controlling rapid maneuvering and fast starting, in analogy with the Strouhal law for steadily flapping foils and the formation number in impulse-started jets.
5. The interaction of foils with oncoming, externally generated vorticity: the three parameters affecting flapping foil interaction with oncoming vorticity are (i) timing of arrival of oncoming eddies, in accordance with vortex-to-vortex interaction laws; (ii) chord size to vortex size, which must be of order one; (iii) frequency matching between foil frequency and vortex frequency of arrival.
6. The influence of Reynolds number on flapping foil performance: the Reynolds number Re has a small to moderate effect, increasing thrust and, hence, efficiency as Re increases.
7. Scaling effects of flexing stiffness of foils: chordwise flexibility can have a significant beneficial effect on propulsive efficiency; measured to be up to 38%. The nondimensional flexibility parameter Δ defined in Eq. (9) must have a value around $1/3$ for optimal efficiency.
8. Scaling laws in fishlike swimming: for fishlike swimming, employing a traveling wave along the body and flapping caudal fin, the principal parameters are the same as for flapping foils (Strouhal number, angle of attack, amplitude of motion-to-chord length ratio); in addition, the phase speed of the traveling wave along the body must exceed the forward velocity—not only to produce thrust by body action, but also to minimize turbulence in the boundary layer.

Acknowledgments

Support by NAVSEA, the Office of Naval Research (Dr. T. McMullen and Dr. P. Bandyopadhyay, monitors), and by the MIT Sea Grant Program is gratefully acknowledged.

References

[1] Videler, J., 1993, *Fish Swimming*, Chapman and Hall, London.
[2] Fish, F. E., and Hui, C. A., 1991, "Dolphin Swimming—A Review," Mammal Rev., **21**, pp. 181–195.
[3] Stamhuis, E., and Videler, J., 1995, "Quantitative Flow Analysis Around Aquatic Animals Using Laser Sheet Particle Image Velocimetry," J. Exp. Biol., **198**, pp. 283–294.
[4] Anderson, J. M., 1996, "Vortex Control for Efficient Propulsion," Ph.D. thesis, Joint Program, MIT and WHOI, Cambridge, MA.
[5] Mueller, U., van den Heuvel, B., Stamhuis, E., and Videler, J., 1997, "Fish Foot Prints: Morphology and Energetics of the Wake Behind a Continuously Swimming Mullet (Chelon Labrosus Risso)," J. Exp. Biol., **200**, pp. 2893–2806.
[6] Wolfgang, M. J., Anderson, J. M., Grosenbaugh, M. A., Yue, D. K. P., and Triantafyllou, M. S., 1999, "Near-Body Flow Dynamics in Swimming Fish," J. Exp. Biol., **202**, pp. 2303–2327.
[7] Drucker, E. G., and Lauder, G. V., 1999, "Locomotor Forces on a Swimming Fish: Three Dimensional Vortex Wake Dynamics Quantified Using DPIV," J. Exp. Biol., **202**, pp. 2393–2412.
[8] Drucker, E. G., and Lauder, G. V., 2001, "Locomotor Function of the Dorsal Fin in Teleost Fishes: Experimental Analysis of the Wake Forces in Sunfish," J. Exp. Biol., **204**, pp. 2943–2958.
[9] Lauder, G. V., 2000, "Function of the Caudal Fin During Locomotion in Fishes: Kinematics, Flow Visualization and Evolutionary Patterns," Am. Zool., **40**, pp. 101–122.
[10] Lighthill, J., 1975, *Mathematical Biofluiddynamics*, SIAM, Philadelphia.
[11] Wu, T., 1961, "Swimming of a Waving Plate," J. Fluid Mech., **10**, pp. 321–344.
[12] Wu, T., 1971, "Hydromechanics of Swimming Propulsion," J. Fluid Mech., **46**, pp. 337–355.
[13] Liu, H., and Kawachi, K., 1998, "A Numerical Study of Insect Flight," J. Comput. Phys., **146**, pp. 124–156.
[14] Cheng, H. K., and Murillo, L. E., 1984, "Lunate-Tail Swimming Propulsion as a Problem of Curved Lifting Line in Unsteady Flow, Part 1: Asymptotic Theory," J. Fluid Mech., **143**, pp. 327–350.
[15] Karpouzian, G., Spedding, G., and Cheng, H. K., 1990, "Lunate-Tail Swimming Propulsion, Part 2: Performance Analysis," J. Fluid Mech., **210**, pp. 329–351.
[16] McCune, J. E., and Tavares, T. S., 1993, "Perspective: Unsteady Wing Theory—The Kármán/Sears Legacy," ASME J. Fluids Eng., **115**(4), pp. 548–560.
[17] Streitlien, K., and Triantafyllou, M. S., 1995, "Force and Moment on a Joukowski Profile in the Presence of Point Vortices," AIAA J., **33**(4), pp. 603–610.
[18] Streitlien, K., Triantafyllou, G. S., and Triantafyllou, M. S, 1996, "Efficient Foil Propulsion Through Vortex Control," AIAA J., **34**(11), pp. 2315–2319.
[19] Ramamurti, R., and Sandberg, W. C., 2001, "Simulation of Flow About Flapping Airfoils Using a Finite Element Incompressible Flow Solver," AIAA J., **39**, pp. 253–260.
[20] Ramamurti, R., and Sandberg, W. C., 2002, "A Three-dimensional Computational Study of the Aerodynamic Mechanisms of Insect Flight," J. Exp. Biol., **205**, pp. 1507–1518.
[21] Guglielmini, L., and Blondeaux, P., 2004, "Propulsive Efficiency of Oscillating Foils," *European Journal of Mechanics/B Fluids* (in the press).
[22] Guglielmini, L., Blondeaux, P., and Vittori, G., 2004, "A Simple Model of Propulsive Oscillating Foils," Ocean Eng. **31**(7), pp. 883–899.
[23] Lewin, G. C., and Haj-Hariri, H., 2003, "Modeling Thrust Generation of a Two-Dimensional Heaving Airfoil in a Viscous Flow," J. Fluid Mech., **492**, pp. 339–362.
[24] Von Ellenrieder, K. D., Parker, K., and Soria, J., 2003, "Flow Structures Behind a Heaving and Pitching Finite-Span Wing," J. Fluid Mech., **490**, pp.

129–138.
[25] Scherer, J. O., 1968, "Experimental and Theoretical Investigation of Large Amplitude Oscillating Foil Propulsion Systems," U.S. Army Engineering Research and Development Laboratories.
[26] DeLaurier, J. D., and Harris, J. M., 1982, "Experimental Study of Oscillating Wing Propulsion," J. Aircr., **19**(5), pp. 368–373.
[27] Lai, P. S. K., Bose, N., and McGregor, R. C., 1993, "Wave Propulsion From a Flexible-Armed, Rigid-Foil Propulsor," Mar. Technol. Soc. J., **30**(1), pp. 28–36.
[28] Anderson, J. M., Streitlien, K., Barrett, D. S., and Triantafyllou, M. S., 1998, "Oscillating Foils of High Propulsive Efficiency," J. Fluid Mech., **360**, pp. 41–72.
[29] Read, D. A., 2001, "Oscillating Foils for Propulsion and Maneuvering of Ships and Underwater Vehicles," SM thesis, MIT, Cambridge, MA.
[30] Ohashi, H., and Ishikawa, N., 1972, "Visualization Study of Flow Near the Trailing Edge of an Oscillating Airfoil," Bull. JSME, **15**(85), pp. 840–847.
[31] Oshima, Y., and Oshima, K., 1980, "Vortical Flow Behind an Oscillating Foil," in *Proc. 15th Int. Congress*, Int. Union Theor. Applied Mech., North Holland, Amsterdam, pp. 357–368.
[32] Oshima, Y., and Natsume, A., 1980, "Flow Field Around an Oscillating Foil," in *Flow Visualization II, Proc. 2nd Int. Symp. on Flow Visualization*, Bochum, Germany, W. Merzkirch (ed.), Hemisphere Publishing, New York, pp. 295–299.
[33] Koochesfahani, M., 1989, "Vortical Patterns in the Wake of an Oscillating Foil," AIAA J., **27**, pp. 1200–1205.
[34] Freymuth, P., 1988, "Propulsive Vortical Signature of Plunging and Pitching Airfoils," AIAA J., **26**, pp. 881–883.
[35] Freymuth, P., 1989, "Visualizing the Connectivity of Vortex Systems for Pitching Wings," ASME J. Fluids Eng., **111**, pp. 217–220.
[36] Freymuth, P., 1990, "Thrust Generation by an Airfoil in Hover Modes," Exp. Fluids, **9**, pp. 17–24.
[37] Freymuth, P., 1991, "Physical Vortex Visualization as a Reference for Computer Simulation," in *Vortex Methods and Vortex Motion*, K. E. Gustafson and J. A. Sethian (eds.), SIAM, Philadelphia, pp. 65–94.
[38] Jones, K. D., Dohring, C. M., and Platzer, M. F., 1998, "Experimental and Computational Investigation of the Knoller-Betz Effect," AIAA J., **36**(7), pp. 1240–1246.
[39] Triantafyllou, M. S., Triantafyllou, G. S., and Gopalkrishnan, R., 1991, "Wake Mechanics for Thrust Generation in Oscillating Foils," Phys. Fluids, **3**(12), pp. 2835–2837.
[40] Triantafyllou, G. S., Triantafyllou, M. S., and Grosenbaugh, M. A., 1993, "Optimal Thrust Development in Oscillating Foils with Application to Fish Propulsion," J. Fluids Struct., **7**, pp. 205–224.
[41] Triantafyllou, M. S., Triantafyllou, G. S., and Yue, D. K. P., 2000, "Hydrodynamics of Fish Swimming," Annu. Rev. Fluid Mech., **32**, pp. 33–53.
[42] Fish, F. E., 1997, "Biological Designs for Enhanced Maneuverability: Analysis of Marine Mammal Performance," *10th Int. Symp. Unmanned Untethered Submersible Technology*, Special Session on Bio-Engineering Research Related to AUV, Durham, NH, pp. 109–117.
[43] Rohr, J. J., and Fish, F. E., 2004, "Strouhal Numbers and optimization by Odontocete Cetaceans," J. Exp. Biol., **207**, pp. 1633–1642.
[44] Nauen, J. C., and Lauder, G. V., 2002, "Hydrodynamics of Caudal Fin Locomotion by Chub Mackerel Scomber Japonicus (Scombridae)," J. Exp. Biol., **205**, pp. 1709–1724.
[45] Motani, R., 2002, "Scaling Effects in Caudal Fin Propulsion and the Speed of Ichthyosaurs," Nature (London), **415**, pp. 309–312.
[46] Taylor, G. K., Nudds, R. L., and Thomas, A. L. R., 2003, "Flying and Swimming Animals Cruise at a Strouhal Number Tuned for High Power Efficiency," Nature (London), **425**, pp. 707–711.
[47] Reynolds, W. C., and Carr, L. W., 1985, "Review of Unsteady, Driven, Separated Flows," AIAA Paper No. 85-0527.
[48] McCroskey, W. J., 1982, "Unsteady Airfoils," Annu. Rev. Fluid Mech., **14**, pp. 285–311.
[49] Maxworthy, T., 1981, "The Fluid Dynamics of Insect Flight," Annu. Rev. Fluid Mech., **13**, pp. 329–350.
[50] Ellington, C. P., 1984, "The Aerodynamics of Hovering Insect Flight," Philos. Trans. R. Soc. London, Ser. B, **305**, pp. 17–181.
[51] Ellington, C. P., Vanderberg, C., Wilmott, A., and Thomas, A., 1996, "Leading Edge Vortices in Insect Flight," Nature (London), **384**, pp. 626–630.
[52] Dickinson, M. H., 1994, "The Effect of Wing Rotation on Unsteady Aerodynamic Performance at Low Reynolds Numbers," J. Exp. Biol., **192**, pp. 179–206.
[53] Dickinson, M. H., Lehmann, F. O., and Sane, S. P., 1999, "Wing Rotation and the Aerodynamic Basis Insect Flight," Science, **284**, pp. 1954–1960.
[54] Walker, J. A., 2003, "Rotational Lift: Something Different or More of the Same?," J. Exp. Biol., **205**, pp. 3783–3792.
[55] Maresca, C., Favier, D., and Rebont, J., 1979, "Experiments on an Airfoil at High Angle of Incidence in Longitudinal Oscillations," J. Fluid Mech., **92**, pp. 671–690.
[56] Ohmi, K., Coutanceau, M., Loc, T. P., and Dulieu, A., 1990, "Vortex Formation Around an Oscillating and Translating Airfoil at Large Incidences," J. Fluid Mech., **211**, pp. 37–60.
[57] Ohmi, K., Coutanceau, M., Daube, O., and Loc, T. P., 1991, "Further Experiments on Vortex Formation Around an Oscillating and Translating Airfoil at Large Incidences," J. Fluid Mech., **225**, pp. 607–630.
[58] Hart, D. P., Acosta, A., and Leonard, A., 1992, "Observations of Cavitation and Wake Structure of Unsteady Tip Vortex Flows," *Proc. Int. STG Symp. Propulsors and Cavitation*, Hamburg, Germany, pp. 121–127.
[59] Ahlborn, B., Harper, D., Blake, R., Ahlborn, D., and Cam, M., 1991, "Fish Without Footprints," J. Theor. Biol., **148**, pp. 521–533.
[60] Lai, J. C. S., and Platzer, M. F., 1998, "The Jet Characteristics of a Plunging Airfoil," *Paper AIAA-98-0101, 36th AIAA Aerospace Sciences Meeting*, Reno, NV.
[61] Guglielmini, L., 2004, "Modeling of Thrust Generating Foils," Ph.D. thesis, University of Genova, Italy.
[62] Strouhal, V., 1878, "Uber Eine Besondere Art der Tonerregung," Ann. Phys. Chem., **5**(10), pp. 216–251.
[63] Zhu, Q., Wolfgang, M. J., Yue, D. K. P., and Triantafyllou, M. S., 2002, "Three-Dimensional Flow Structures and Vorticity Control in Fish-Like Swimming," J. Fluid Mech., **468**, pp. 1–28.
[64] Hover, F. S., Haugsdal, O., and Triantafyllou, M. S., 2003, "Control of Angle of Attack Profiles in Flapping Foil Propulsion," J. Fluids Struct., **19**, pp. 37–47.
[65] Gursul, I., Lin, H., and Ho, C. M., 1991, "Vorticity Dynamics of 2D and 3D Wings in Unsteady Free Stream," AIAA Paper 91-0010, Reno, NV.
[66] Cheng, J.-Y., Zhuang, L.-X., and Tong, B.-G., 1991, "Analysis of Swimming Three-Dimensional Waving Plates," J. Fluid Mech., **232**, pp. 341–355.
[67] Martin, C. B., 2001, "Propulsive Performance of a Rolling and Pitching Wing," MS thesis, Massachusetts Institute of Technology.
[68] Martin, C. B., Hover, F. S., and Triantafyllou, M. S., 2001, "Propulsive Performance of a Rolling and Pitching Wing," *Proc. UUST*, Durham, NH.
[69] Kato, N., 1998, "Locomotion by Mechanical Pectoral Fins," J. Mar. Sci. Technol., **3**, pp. 113–121.
[70] Kato, N., and Inaba, T., 1997, "Hovering Performance of Fish Robot With Apparatus o Pectoral Fin Motion," *10th Int. Symp. on Unmanned Untethered Submersible Technology*, University of New Hampshire.
[71] Kato, N., 2000, "Control Performance of Fish Robot With Mechanical Pectoral Fins in Horizontal Plane," IEEE J. Ocean. Eng., **25**(1), pp. 121–129.
[72] Walker, J. A., and Westneat, M. W., 2000, "Mechanical Performance of Aquatic Rowing and Flying," Proc. R. Soc. London, Ser. B, **267**, pp. 1875–1881.
[73] Culik, B. M., Wilson, R. P., and Bannasch, R., 1994, "Underwater Swimming at Low Energetic Cost by Pygoscelid Penguins," J. Exp. Biol., **197**, pp. 65–78.
[74] Bandyopadhyay, P., Donnelly, M. J., Nedderman, W. H., and Castano, J. M., 1997b, "A Dual Flapping Foil Maneuvering Device for Low-Speed Rigid Bodies," *Third Int. Symp. Performance Enhancement for Marine Vehicles*, Newport, RI.
[75] Czarnowski, J. T., 1997, "Exploring the Possibility of Placing Traditional Marine Vessels Under Oscillating Foil Propulsion," SM thesis, Dept. Ocean Eng., Massachusetts Institute of Technology, Cambridge, MA.
[76] Tsuhara, M., and Kimura, T., 1987, "An Application of the Weis-Fogh Mechanism to Ship Propulsion," ASME J. Fluids Eng., **109**, pp. 107–13.
[77] Weis-Fogh, T., 1973, "Quick Estimates of Flight Fitness in Hovering Animals Including Novel Mechanisms for Lift Production," J. Exp. Biol., **59**, pp. 169–230.
[78] Bandyopadhyay, P. R., Castano, J. M., Donnelly, M. J., Nedderman, W. H., and Donnelly, M. J., 2000, "Experimental Simulation of Fish-Inspired Unsteady Vortex Dynamics on a Rigid Cylinder," ASME J. Fluids Eng., **122**, pp. 219–238.
[79] Webb, P. W., 1997, "Designs for Stability and Maneuverability in Aquatic Vertebrates: What Can We Learn," *Proc. 10th Int. Symp. Unmanned Untethered Submersible Technology*, Durham, NH, pp. 86–108.
[80] Webb, P. W., 2000, "Maneuverability Versus Stability: Do Fish Perform Well in Both?," *Proc. 1st Int. Symp. On Aqua Bio-Mechanisms (ISBMEC 2000)*, Honolulu, Hawaii.
[81] Harper, D. G., and Blake, R. W., 1991, "Prey Capture and the Fast-Start Performance of Northern Pike (Esox Lucius)," J. Exp. Biol., **155**, pp. 175–192.
[82] Frith, H. R., and Blake, R. W., 1995, "Mechanical Power Output and Hydrodynamical Efficiency of Northern Pike (Esox Lucius) Fast-Starts," J. Exp. Biol., **198**, pp. 1863–1873.
[83] Triantafyllou, M. S., Techet, A. H., Zhu, Q., Beal, D. N., Hover, F. S., and Yue, D. K. P., 2003, "Vorticity Control in Fish-Like Propulsion and Maneuvering," Integr. Comp. Biol., **42**(5), pp. 1026–1031.
[84] Read, D. A., Hover, F. S., and Triantafyllou, M. S., 2003, "Forces on Oscillating Foils for Propulsion and Maneuvering," J. Fluids Struct., **17**, pp. 163–183.
[85] Kato, N., 1999, "Hydrodynamic Characteristics of Mechanical Pectoral Fin," ASME J. Fluids Eng., **121**, pp. 605–613.
[86] Kato, N., 1999, "Three-Motor-Driven Mechanical Pectoral Fin," *Proc. 11th Int. Symp. Unmanned Untethered Submersible Technology*, Durham, NH, pp. 467–476.
[87] Hertel, H., 1966, *Structure Form and Movement*, Reinhold, New York.
[88] Flores, M. D., 2003, "Flapping Motion of a Three-Dimensional Foil for Propulsion and Maneuvering of Underwater Vehicles," S.M. thesis, Dept. Ocean Engineering, MIT, Cambridge, MA.
[89] Triantafyllou, M. S., Zhu, Q., Techet, A. H., and Yue, D. K. P., 2003, "Scaling Law in Rapidly-Maneuvering Fish," *56th Annual Meeting, Division of Fluid Dynamics, American Physical Society*, East Rutherford, NJ.
[90] Daigh, S., and Techet, A. H., 2003, "Experimental Visualization of Rapidly Maneuvering Fish," *56th Annual Meeting, Division of Fluid Dynamics*, E. Rutherford, NJ.
[91] Gharib, M., Rambod, E., Dabiri, D., and Hammache, M., 1994, "Pulsatile Heart Flow: A Universal Time Scale," *Proc. 2nd Int. Conf. Experimental Fluid*

Mech., M. Onorato, (ed.) Torino, Italy.
[92] Gharib, M., Rambod, E., and Shariff, K., 1998, "A Universal Time Scale for Vortex Ring Formation," J. Fluid Mech., **360**, pp. 121–140.
[93] Rosenfeld, M., Gharib, M., and Rambod, E., 1998, "Circular and Formation Number of Laminar Vortex Rings," J. Fluid Mech., **376**, pp. 297–318.
[94] Isshiki, H., and Murakami, M., 1984, "A Theory of Wave Devouring Propulsion," J. Soc. Naval Arch. Jpn, **156**, pp. 102–114.
[95] Sparenberg, J. A., and Wiersma, A. K., 1975, "On the Efficiency Increasing Interaction of Thrust Producing Lifting Surfaces," in *Swimming and Flying in Nature*, Plenum Press, T. Wu, C. J. Brokaw, and C. Brennen, (eds.) Vol. 2, pp. 891–917.
[96] Koochesfahani, M., and Dimotakis, P., 1998, "A Cancellation Experiment in a Forced Turbulent Shear Layer," AIAA Technical Paper 88-3713-CP.
[97] Gopalkrishnan, R., Triantafyllou, M. S., Triantafyllou, G. S., and Barrett, D. S., 1994, "Active Vorticity Control in a Shear Flow Using a Flapping Foil," J. Fluid Mech., **274**, pp. 1–21.
[98] Beal, D. N., Hover, F. S., and Triantafyllou, M. S., 2001, "The Effect on Thrust and Efficiency of an Upstream Karman Wake on an Oscillating Foil," *Proc. UUST*, Durham, NH.
[99] Liao, J. C., Beal, D. N., Lauder, G. V., and Triantafyllou, M. S., 2003, "The Karman Gait: Novel Body Kinematics of Rainbow Trout Swimming in a Vortex Street," J. Exp. Biol., **206**, pp. 1059–1073.
[100] Liao, J. C., Beal, D. N., Lauder, G. V., Triantafyllou, M. S., 2003, "Fish Exploiting Vortices Use Less Muscle," Science, **302**, pp. 1566–1569.
[101] Hoerner, S. F., 1965, *Fluid Dynamic Drag* (published by the author).
[102] Bose, N., 1995, "Performance of Chordwise Flexible Oscillating Propulsors Using A Time-Domain Panel Method," Int. Shipbuild. Progr., **42**(432), pp. 281–294.
[103] Castelo, M. E., 2002, "Propulsive Performance of Flexible-Chord Foils," B.S. thesis, Department of Ocean Engineering, MIT.
[104] Prempraneerach, P., Hover, F. S., and Triantafyllou, M. S., 2003, "The Effect of Chordwise Flexibility on the Thrust and Efficiency of a of Flapping Foil" *Proceedings Unmanned, Untethered Submersible Technology*, Durham, NH, Aug.
[105] Liu, P., and Bose, N., 1997, "Propulsive Performance From Oscillating Propulsors With Spanwise Flexibility," Proc. R. Soc. London, Ser. A, **453**, pp. 1763–1770.
[106] Katz, J., and Weihs, D., 1979, "Large Amplitude Unsteady Motion of a Flexible Slender Propulsor," J. Fluid Mech., **90**, pp. 713–723.
[107] McCutchen, C. W., 1970, "The Trout Tail Fin: A Self-Cambering Hydrofoil," J. Biomech., **3**, 271–281.
[108] Combs, S. A., and Daniel, T. L., 2001, "Shape, Flapping and Flexion: Wing and Fin Design for Forward Flight," J. Exp. Biol., **204**, pp. 2073–2085.
[109] Alexander, R. McN., 2003, *Principles of Animal Locomotion*, Princeton University Press, Princeton, N. J.
[110] Blake, R. W., 1983, *Fish Locomotion*, Cambridge University Press, London.
[111] Clark, B. D., and Bemis, W., 1979, "Kinematics of Swimming of Penguins at the Detroit Zoo," J. Zool., **188**, pp. 411–428.
[112] Triantafyllou, M. S., and Triantafyllou, G. S., 1995, "An Efficient Swimming Machine," Sci. Am., **272**(3), pp. 64–70.
[113] Kumph, J., and Triantafyllou, M. S., 1998, "A Fast-Starting and Maneuvering Vehicle, the Robopike," *Proc. Int. Symp. Seawater Drag Reduction*, Newport, RI.
[114] Techet, A. H., 2001, "Experimental Visualization of the Near-Boundary Hydrodynamics About Fish-Like Swimming Bodies," Ph.D. thesis, MIT, Cambridge, MA.
[115] Techet, A. H., Anderson, E. J., McGillis, W. R., Grosenbaugh, M. A., and Triantafyllou, M. S., 1999, "Flow Visualization of Swimming Robotic Fish in the Near Boundary Region," *Third Int. Workshop on Particle Image Velocimetry*, Santa Barbara, CA, September 16–18, 1999.
[116] Taneda, S., 1977, "Visual Study of Unsteady Separated Flows Around Bodies," Prog. Aerosp. Sci., **17**, pp. 287–348.
[117] Shen, L., Zhang, X., Yue, D. K. P., and Triantafyllou, M. S., 2003, "Turbulent Flow Over a Flexible Wall Undergoing a Streamwise Traveling Wavy Motion," J. Fluid Mech., **484**, pp. 197–221.

Michael S. Triantafyllou *completed undergraduate studies (diploma 1974) in naval architecture and marine engineering at the National Technical University of Athens, graduate studies in ocean engineering at MIT, Cambridge, MA (SM 1977, ScD 1979). He joined the faculty at MIT in 1979. He has taught and published in the areas of dynamics and control of marine systems, experimental fluid mechanics, and biomimetics. Triantafyllou is a member of the Society of Naval Architects & Marine Engineers, the American Physical Society, and the International Society for Offshore & Polar Engineers. Awards include: RoboTuna on permanent exhibit at the Museum of Science, London (since 1998); prototype RoboTuna in national traveling exhibit on robots, Science Museum of Minnesota (2003–2004); Discover Magazine Awards for Technological Innovation (1998); ABS/Linnard Prize for best paper in the Transactions of SNAME (1997); Highlight Paper of 1995, Scientific American; H.L. Doherty Professorship in Ocean Utilization (1983–1985).*

Alexandra H. Techet *received her B.S.E. degree in mechanical and aerospace engineering at Princeton University, Princeton, NJ, USA in 1995, and her MS and PhD degrees in oceanographic engineering from the Massachusetts Institute of Technology (MIT), Cambridge, MA/Woods Hole Oceanographic Institute (WHOI), Woods Hole, MA, joint program in 1998 and 2001, respectively. She joined the faculty in the Ocean Engineering Department at MIT in 2002, as assistant professor, and was awarded the H. L. Doherty Professorship in Ocean Utilization (2002–2004). Her research interests include experimental marine hydrodynamics, ship-breaking waves, fluid-structure interactions, and fishlike swimming and maneuvering. Professor Techet is a member of the American Society of Mechanical Engineers, American Physical Society, Marine Technology Society, and the International Society of Offshore and Polar Engineers.*

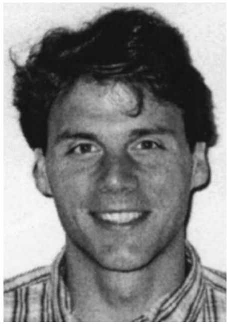

Franz S. Hover *received his B.S. in Mechanical Engineering from Ohio Northern University (Ada, Ohio) in 1987, and his S.M. and Sc.D. degrees in 1989 and 1993 in oceanographic and mechanical engineering from the Woods Hole Oceanographic Institution/Massachusetts Institute of Technology Joint Program. He was a postdoctoral fellow at the Monterey Bay Aquarium Research Institute and has been a regular consultant to industry. He is currently a Principal Research Engineer at the Massachusetts Institute of Technology Department of Ocean Engineering. Areas of research interest include design and applied control of marine systems. Dr. Hover is a member of the American Society of Mechanical Engineers.*

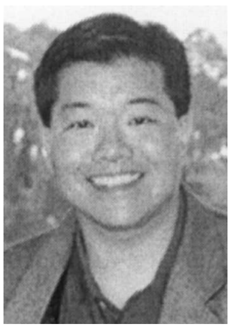

Dick K.P. Yue *is the Associate Dean of Engineering and Professor of Hydrodynamics & Ocean Engineering at MIT. He received his degrees (SB, SM, and ScD) from MIT. He has been a faculty member since 1983. He is active in research and teaching in marine fluid mechanics and ocean engineering, focusing on ocean and coastal wave dynamics, large-amplitude motions of ships and platforms, nonlinear wave mechanics, hydrodynamics of fish swimming, and the application of these principles to the design of underwater vehicles; and vortical and turbulent flows at the air-sea interface, and their effects on interfacial processes. Yue is a member of the Society of Naval Architects & Marine Engineers and the American Physical Society.*